

## Histological, Immunohistochemical and Biochemical Assessment of the Protective Capacity of Cloves Against Furan-induced Submandibular Changes in Adult Male Albino Rats

Hala El-Haroun and Nadia Said Badawy Khair

Department of Histology, Faculty of Medicine, Menoufia University, Egypt

### ABSTRACT

**Background:** Furan is a compound of food pollutants widely dispersed in air, water, soil, and sediments throughout the world. It is present in processed food exposed to heat as canning and pasteurization. It is also found in cigarette smoke and as an intermediate compound in the processing of several chemical and pharmaceutical products. In folk medicine, food flavoring, fragrance and pharmaceuticals, cloves are employed. There are many health benefits of Clove and it sometimes used as an antibacterial, antifungal, antiseptic and antioxidant agent.

**Aim:** The current research examines the impact of furan on the histological structure of adult male albino rats' submandibular salivary glands and tests the feasible protective effect of clove extract.

**Materials and Methods:** Current study has used 48 male albino rats. The rats were randomly divided into four groups: control group, Clove-treated group received 500 mg / kg / day, 5 days / week, Furan-treated group received 8 mg / kg, 5 days / week, and Furan and Clove group, anesthetized and sacrificed at the end of the study (8 weeks). Both animal submandibular glands were excised for histological, histochemical, immunohistochemical and electron microscopy tests. Morphometric study and statistics were conducted.

**Results:** In addition to periductal and perivascular excessive collagen fibers accumulation, Furan treated submandibular glands showed disorganization, degeneration and vacuolation of acinar and ductal cells. Ultrastructural changes in the range of pyknotic nuclei, dilated rough endoplasmic reticulum, degenerated mitochondria followed by loss of infolded basal membrane. Furan increased apoptosis and decreased cytoplasmic CYP2E1. It lowered antioxidant enzymes, superoxide dismutase (SOD) and Catalase (CAT) significantly and simultaneously elevated malondialdehyde (MDA) level. Clove extract administration ameliorated these changes, showing major improvements in submandibular structure.

**Conclusion:** It can well be concluded that cloves can exert a protective effect and reduce toxicity of Furan on submandibular gland.

**Received:** 13 November 2020, **Accepted:** 17 December 2020

**Key Words:** Cloves, CYP2E1, furan, submandibular gland.

**Corresponding Author:** Hala El-Haroun, PhD, Department of Histology, Faculty of Medicine, Menoufia University, Egypt, **Tel.:** +201 0066 01467, **E-mail:** elharoun@yahoo.com

**ISSN:** 1110-0559, Vol. 44, No.4

### INTRODUCTION

Furan is a lucent, flammable evaporative and lipotropic composite used as a transitional component in the manufacture of many chemical and pharmaceutical products, solvents and coatings<sup>[1]</sup>.

In most components of the ecosystem, such as air, water, sediments, and soil, Furan may be a food contaminant compound widely distributed throughout the environment. It is transmitted to animals and preserved for years in adipose tissues, then streams into circulating blood as a result of stress or hunger, and tends to have a noxious effect<sup>[2]</sup>. In addition, furan is a food pollutant that incidentally develops in the preservation of food subjected to heat as canning and pasteurization, being developed as key industrial derivatives. It is also present in cigarette smoke<sup>[3]</sup>.

An extremely large range of furan containing foods, in particular coffee, baby food and canned food items with

levels exceeding 100 ppb, has been found. Furan is also found in an incredibly broad variety of consumed foods, such as wheat, bread, roasted coffee, and cooked meat. The majority of people exposed to furan are taken into account in order to be dietary. There is a higher content of furan in meat, milk products and fish than in fruit, vegetables, and grains<sup>[4]</sup>.

During thermal degradation of food constituents through multiple pathways, furan compounds [polychlorinated dibenzofurans] are formed. Thermal degradation of certain amino acids by cysteine or serine alone causes the formation of furan. While other amino acids need to reduce sugar in order to generate furan, such as aspartic acid, alanine and threonine. Furan may also be produced in the absence of amino acids as a byproduct of sugar degradation<sup>[5]</sup>.

Furan is highly toxic and is connected to significant health problems such as cancer, failure of immunity, hormonal disparity, and knockout of the system, growth rate

and behavioral disruption. In addition to those deleterious postnatal consequences, furan-related developmental disabilities within the fetus are another major concern<sup>[6]</sup>. Experimental animal research has shown that furan is still highly toxic at very low concentrations. Furan and its derivatives are cytotoxic and cause necrosis and death, most commonly in the liver<sup>[7]</sup>, lungs and kidneys<sup>[8]</sup>. They induce skin disorders, damage of the endocrine system, reproductive functions<sup>[9]</sup> and pancreas<sup>[10]</sup>. Furan has been identified as carcinogenic and genotoxic in rats at higher doses. Furan carcinogenicity and toxicity may also be intervening by initiation and acceleration of cytochrome P450<sup>[11]</sup>.

Cloves are the dried flower buds of *Syzygium aromaticum*, which is part of the Myrtaceae family. It is harvested primarily for the unopened flower buds borne in clusters, that are dried to obtain whole clove buds<sup>[12]</sup>. Cloves are used as folk medicine, food flavourings, food preservatives, fragrances and pharmaceuticals, but scientists have only recently begun to research their possible health benefits<sup>[13]</sup>. Other clove products include ground clove, volatile oils derived from clove buds, stem or leaf, and oleoresin. Cloves, commonly associated with periodontal diseases and caries, are known to be effective sources of anti-microbial agents against oral bacteria<sup>[14]</sup>. It contains: eugenol (up to 95%), acetyl eugenol,  $\beta$ -caryophyllene, methyl salicylate, pinene, volatile oil. Clove and clove oil can also be used as an antiseptic, antifungal and antiseptic agent, and the use of clove and oil is expected to extend in line with 'the return to nature'. Various animal studies have shown that compounds in cloves have many health benefits, including promoting the health of the liver and helping to regulate the level of glucose<sup>[15]</sup>. Furthermore, the antioxidant activity of cloves, which enhances food safety, was shown in a recent study<sup>[16]</sup>.

Data on the impact of furan toxicity on the structure of the submandibular gland was very limited. Therefore, the current research was planned to investigate furan's impact on the histological structure of the submandibular salivary glands of male albino rats and, using histological, histochemical and immunohistochemical methods. Also, to determine the potential protective effect of cloves extract against furan-induced submandibular toxicity.

## MATERIALS AND METHODS

### Chemicals

At a dose of 8 mg / kg dissolved in 4 ml / kg corn oil, Furan (CAS no. 110-00-9, 99 percent pure) was administered 5 days / week for 8 weeks by oral gavage<sup>[17]</sup>. As a solvent for furan, corn oil, which is available in the form of an oily solution, was used (Sigma-Aldrich Chemical Company, Saint Louis, Missouri, USA)<sup>[18]</sup>.

### Preparation for Clove Extract

Cloves were harvested (*Eugenia caryophyllata*) and then dried. The arid stuff of the plant was dusted by a grinder. The extraction was carried out at room temperature. In

each solvent, approximately 100 g of dried plant stuff was immersed separately in ethanol, water, and acetone (1 L) for 5-7 days. The immersed material was mixed every 18 hrs with a sterilized glass rod. Through Whatman document No.1, the ultimate extract was filtered. By vacuum evaporation at 40°C, the acquired filtrate was concentrated, and then stored for further use at 4°C. This procedure has been eliminated by the Department of Biochemistry, Faculty of Agriculture, Menoufia University.

### Animals

Forty-eight adult male albino (3-4 months old) rats were employed in this study, each weighing 180-220gm. They were housed in clean stainless-steel cages at average temperature. They had free access to ad-libitum food and water. Strict hygiene and care has been taken to maintain them in a healthy and normal environment. The animals' overall conditions and behavior were noticed. Animal therapy was in line with the ethical protocol approved by the Menoufia Faculty of Medicine Ethical Committee.

### Experimental procedure

The rats were randomly divided into four groups, each of which included 12 animals.

**Group I (control group):** split into two similar subgroups: subgroup Ia (negative control): no treatment obtained and subgroup Ib: Vegetable oil received (4 ml / kg, 5 days / week for 8 weeks).

**Group II (Clove treated group):** clove extract obtained at a dose of 500 mg / kg / day, 5 days / week for 8 weeks by gastric tube<sup>[19]</sup>.

**Group III (Furan treated group):** rats received a dose of 8 mg / kg of Furan, orally dissolved in 4 ml / kg of vegetable oil, 5 days per week for 8 weeks<sup>[17]</sup>.

**Group IV (Group of Furan and Clove extracts):** obtained Furan at 8 mg / kg gavage dose concurrently with Clove extract at 500 mg / kg gastric tube dose, 5 days / week for 8 weeks. Animals from all groups were anaesthetized and sacrificed at the end of the study (8 weeks). Both animals' submandibular glands were both excised and processed for histological, histochemical, immunohistochemical and transmission microscopy examination.

### I-Histological study

In 10% of formal saline washed and processed for paraffin sections, tissue samples have been fixed. Sections of about 5-6  $\mu$ m thickness were obtained and stained by Hematoxylin and eosin (Hx&E) to show the histological structure and Mallory trichrome stain of to detect collagen fibers<sup>[20]</sup>.

### II-Histochemical study

Periodic Acid Schiff-Alcian Blue (PAS-AB) stain for glycogen and mucopolysaccharide inspection. Dewaxed parts in xylene, then rehydrated and stained for 30 minutes

with Alcian-blue solution, followed by periodic acid oxidation. Sections were then coated with Schiff's reagent for 15 minutes and sections were finally dehydrated, washed and mounted with Canadian balsam<sup>[21]</sup>.

### III-Immunohistochemical study

The peroxidase-labelled technique for Streptavidin-Biotin was used<sup>[22]</sup>. Anti-Caspase-3 (Dilution 1/50 rabbit polyclonal antibody, Thermo Scientific, Fermont, CA 94539, USA) and anti-cytochrome P450 2E1 (Dilution 1:500 rabbit polyclonal antibody, CYP2E1, Abcam, Cairo, Egypt, Catalog No ab53945) were used. With the diluted primary antibody using PBS, the slides were incubated. Consequently, drops of streptavidin peroxidase were added to the slide. Then slides were stained with chromogen diaminobenzidine (DAB), counterstained with hematoxylin then dehydrated and placed. Negative controls were processed in identical steps except for primary antibody use<sup>[23]</sup>. Tonsil tissue for Caspase-3 and hepatic Carcinoma for CYP2E1 were used as positive control.

### IV-Transmission Electron microscopic analysis

Submandibular gland specimens were cut and left in 3% glutaraldehyde for twenty-four h with 0.1 mol / l PBS at 4 ° C for transmission electron microscope (TEM) processing. The sections are dehydrated in an incredibly large series of ethanol rinses, then washed with propylene oxide and inserted in the epon. Semi-thin sections were cut and stained with toluidine blue. Ultrathin sections with uranyl acetate and lead citrate were cut and stained. Under the Jeol electron microscope, the ultra-structure of the tissues was studied<sup>[24]</sup>. At the Electron Microscopy Facility, Faculty of Medicine, Tanta University, TEM processing and analysis were performed.

### V-Biochemical analysis

Submandibular salivary gland tissues were extracted, homogenized in 1 ml PBS, pH 7.4 and centrifuged at 4500 rpm for 15 min at 4 ° C for the determination of the antioxidant enzymes, after which the supernatant was collected for the assessment of malondialdehyde (MDA)<sup>[25]</sup>, Catalase (CAT)<sup>[26]</sup> and superoxide dismutase (SOD)<sup>[27]</sup> using a spectrophotometer.

### VI-Study of histomorphometrics and statistical analysis

The "Leica Qwin 500 C" image analyzer automated data processing system Ltd. (Cambridge, England) was used to collect all the quantitative data. At magnification of 400, 10- non-overlapping fields taken from 10 slides of each rat were randomly used to determine the area percentage (percent) of collagen fibers in Mallory trichrome stained sections within the groups studied. Histomorphometric measurement data and biochemical results were analysed and contrasted using the student t-test. In contrast to the control group, the *P-value* was used to evaluate the various changes in and parameter within the experimental animals. The data collected was tabulated as mean  $\pm$  variance (SD)

and analyzed using the Science Discipline Software (SPSS) statistical package (version 17.0 on an IBM compatible computer; SPSS Inc., Chicago, Illinois, USA). *P* was non-significant at 0.05, *P* > 0.05; *P* < 0.05 was significant, while *P* < 0.001 was extremely significant<sup>[28]</sup>.

## RESULTS

### Light microscopic results

In H& E sections, the submandibular salivary gland of control albino rats (groups I & II) showed the general normal histological architecture of the foremost salivary glands without any difference between them. The gland consisted of serous, mucous and mixed acini with excretory ducts. The mixed acini formed of mucous acini and serous demilunes (Figures 1,2). The mucous acini had narrow lumen and lined by pyramidal cells with faint foamy cytoplasm and basal flat to oval nuclei. The serous acini had darkly stained cytoplasm and central rounded basophilic nuclei. Serous demilunes appeared as crescent on some mucous acini. The intercalated duct lined by cuboidal epithelium with central round nuclei and eosinophilic cytoplasm (Figure 2). However, Furan- treated (group III) rats 'submandibular salivary glands displayed disorganized degenerated acini, vacuolations of cells of the interlobular ducts, periductal cellular infiltration and congested blood vessel (Figure 3). Many distorted serous acini and mucous acini with degenerated cells were seen (Figures 4,5). The cells of some mucous acini had no nuclei and others had desquamated nuclei in their lumen (Figure 4). Apparent decrease in mucous acini was observed (Figure 5). The distorted acini contained several cytoplasmic vacuolations, swollen hyperchromatic nuclei and hemorrhagic spots (Figure 6).

On the other hand, analysis of the rat treated with furan + Clove extract (group IV) showed a marked decrease in the pathological changes of the gland. H&E stained sections showed that the gland restored its general architecture, which was quite as in control animals. Regular acinar patterns with normal acini and duct system were evidently present (Figures 7,8). However, few desquamated nuclei in lumen of some mucous acini were still present (Figure 7)

Mallory Trichrome stained submandibular salivary gland sections of control groups (group I & II) displayed thin connective tissue capsule and small amount of collagen fibres around the acini and even the ducts (Figure 9). Excessive periductal and perivascular accumulation of collagen fibers was revealed in rats of the Furan-treated group (group III) (Figure 10). Furan + Clove extract treated rats (group IV) showed moderate deposition of collagen fibers around the ducts and the acini (Figure 11).

Alcian blue-PAS staining of the control group submandibular salivary gland demonstrated a clear PAS + ve reaction of the serous acini and duct cells, while the mucous acini had a strong blue Alcian reaction (Figure 12). The serous acini's weak PAS + ve reaction was shown by

the Furan treated group. Moderate Alcian blue + ve mucus acini reaction and weak Alcian blue + ve duct reaction were seen (Figure 13). Furthermore, the Furan & Clove extract group showed moderate to strong PAS + ve serous acini and duct reaction, while the mucous acini showed moderate Alcian blue + ve reaction (Figure 14).

**Anti-Caspase-3 immunohistochemical staining:**Control group revealed negative anti-Caspase immunoreactivity in acinar cells (Figure 15). Sections of the Furan treated group revealed strong positive nuclear anti-Caspase immune reaction in most acinar cells (Figure 16), while sections of the Furan & clove extract group exhibited negative anti-Caspase immune reaction more or less as in control group (Figure 17).

**Anti-CYP2E1:**In sections of the control group, expression revealed strong positive cytoplasmic anti-CYP2E1 expression in acini (Figure 18). The group treated with furan showed mild positive expression of cytoplasmic anti-CYP2E1 in acini (Figure 19). However, a moderate positive cytoplasmic anti-CYP2E1 acini immune response was seen in the Furan & clove extract sections (Figure 20).

### Electron microscopic results

Serous secreting acinar cells having regular euchromatic nuclei, basal and perinuclear cisterns of rough endoplasmic reticulum and supranuclear homogenous electron-dense secretory granules were revealed by electron microscopic analysis of rat submandibular glands of control groups (Groups I & II) (Figure 21). Regarding the mucous acinus cell, there was basal oval nucleus, basal cisternae of rough endoplasmic reticulum and apical secretory granules. Their secretory granules were electron-lucent and having variable sizes and filling most of the cytoplasm (Figure 22). The basal part of the striated duct cell had rounded euchromatic nucleus, basal membrane infoldings and mitochondria in between (Figure 23).

Regarding furan-treated animals (group III), ultrastructural changes were observed in the secretory cells and ductal cells. Serous acinar cells showed more condensed nuclear chromatin, dilated perinuclear space, dilated cisternae of rough endoplasmic reticulum and degenerated mitochondria. The secretory granules were morphologically heterogenous and showed apparent decrease in many sections. Some contents appeared dense while others were lucent (Figures 24,25). Mucous acinar cell had vacuolated cytoplasm, irregular indented nucleus, and dilated cisternae of rough endoplasmic reticulum (Figure 26). Basal migration of the secretory granules was a prominent feature in most of secretory cells (Figure 27). The striated duct cells showed loss of normal architecture. Multiple cytoplasmic vacuoles, apical pinocytotic vesicles with loss of basal membrane infoldings in the striated duct cells were observed (Figure 28).

Examination of ultrathin sections of Furan +Clove extract treated rat (group IV) was nearly the same as that of the control group. Serous acinar cells with euchromatic regular nuclei, and apical dense secretory granules with intact intercellular junctions were seen. However, rough endoplasmic reticulum in few cells showed mild dilatation (Figure 29). The mucous acinar cells showed nearly regular nuclei with perinuclear and basal rough endoplasmic reticulum cisternae, and electron lucent supranuclear secretory granules. Some cisternae of rough endoplasmic reticulum still dilated (Figure 30). The striated duct cell had an euchromatic nucleus, almost regular infoldings with presence of mitochondria in between (Figure 31).

### Biochemical results

The data in table (1) showed a non-significant ( $P>0.05$ ) difference between group I&II within the normal tissue level of MDA (the marker of lipid peroxidation). However, the treatment with Furan showed a highly significant increase ( $p < 0.001$ ) in the MDA level relative to the control group animals. In Furan treated rats (group III), however, a highly significant ( $p < 0.001$ ) decrease in the activity of antioxidant enzymes was observed; catalase (CAT) and enzyme (SOD) were observed. In contrast, treated rats with Furan and Clove extract (group IV) showed a highly significant ( $p < 0.001$ ) reduction in MDA and a highly significant increase ( $P<0.05$ ) in antioxidant status (SOD, CAT) compared to treated rats with Furan (group III) (Histograms 1,2,3 and Table 1).

### Histomorphometric and statistical analysis

In contrast to the control group (group I), Furan-treated rats (group III) showed a highly significant increase ( $P<0.001$ ) in the mean area percentage (percent) of collagen fibers content. On the other hand, Furan + Clove extract treated rats (group IV) showed a highly significant decrease ( $P<0.001$ ) compared to Furan-treated rats (group III) (Histogram 4 and Table 2).

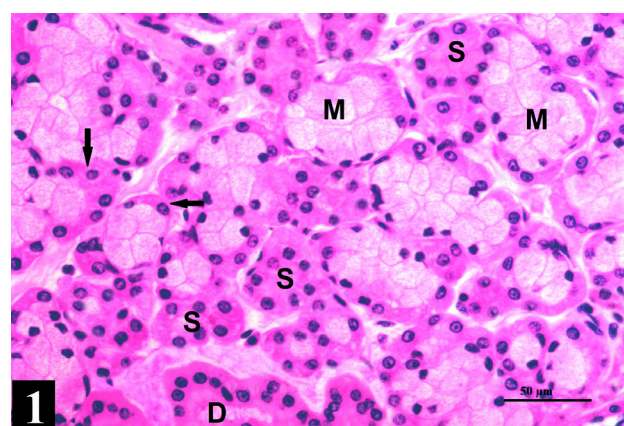


**Fig. 1:** A photomicrograph of a section of submandibular gland from a control rat (group I) showing serous acini (S), large pale staining mucous acini (M). Serous demilunes (arrows) and excretory ducts (D) are present. (H&E x 200).

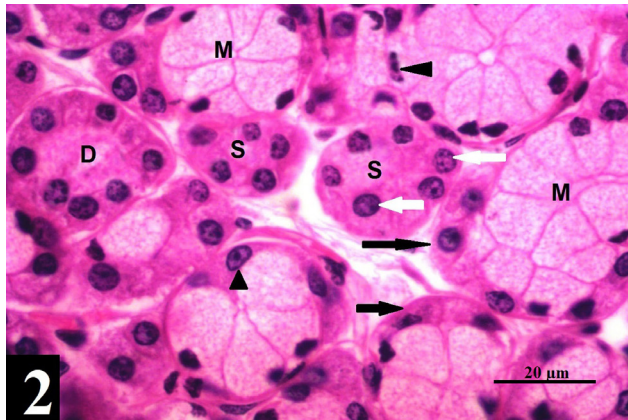


**Fig. 2:** A photomicrograph of a section of submandibular gland from a control rat (group I) showing mucous acini having narrow lumen and lined by pyramidal cells with faint foamy cytoplasm (M) and basal flat to oval nuclei (arrow head). The serous acini have darkly stained cytoplasm (S) and central rounded basophilic nuclei (white arrow). Serous demilunes appeared as crescent on some mucous acini [black arrow]. The intercalated duct lined by cuboidal epithelium with central round nuclei and eosinophilic cytoplasm (D). (H&E x 400).

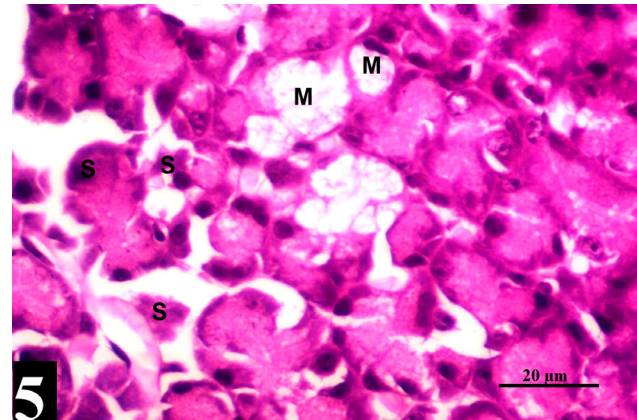


**Fig. 5:** A photomicrograph of a section of submandibular gland from a furan treated rat [group III] showing distorted serous acini [S] and mucous acini with apparent decrease in mucous acini. [H&E x 400]

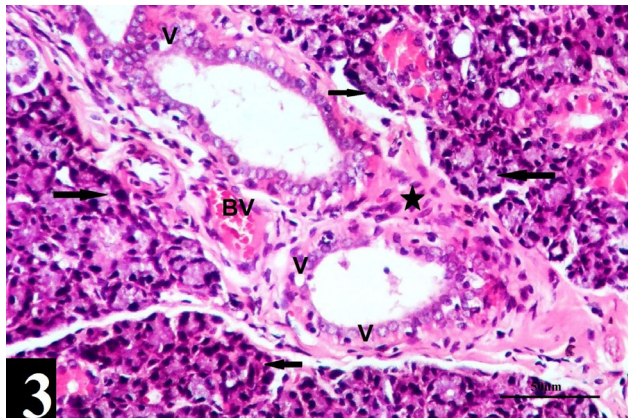


**Fig. 3:** A photomicrograph of a section of submandibular gland from a furan treated rat (group III) showing disorganized degenerated acini (arrows), interlobular duct cell vacuolations (V), periductal cell infiltration (star) and congested blood vessels (BV). (H&E x 200).

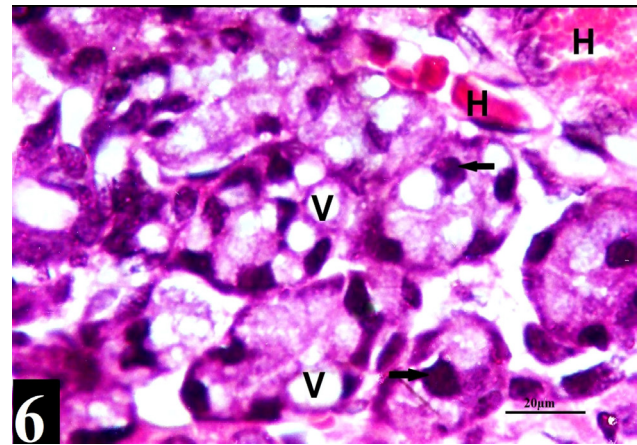


**Fig. 6:** A photomicrograph of a section of submandibular gland from a furan treated rat (group III) showing distorted serous acini containing multiple intracytoplasmic vacuoles (V) and enlarged hyperchromatic nuclei (arrow). Note hemorrhagic spots (H) are present. (H&E x 400).

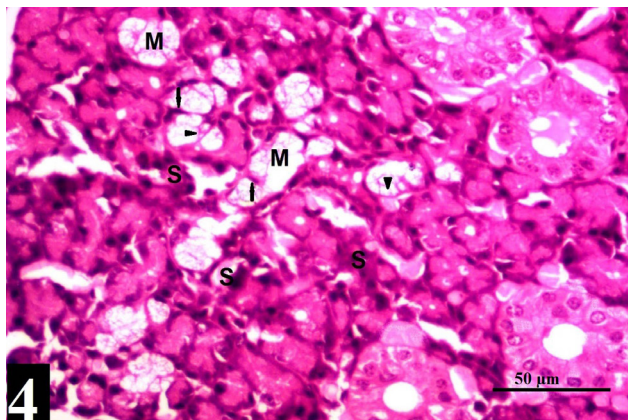


**Fig. 4:** A photomicrograph of a section of submandibular gland from a furan treated rat (group III) showing distorted serous acini (S) and mucous acini with degenerated cells (M) were seen. Notice some cells of mucous acini have no nuclei (arrow head) and others have desquamated nuclei (arrow) in the lumen. (H&E x 200).

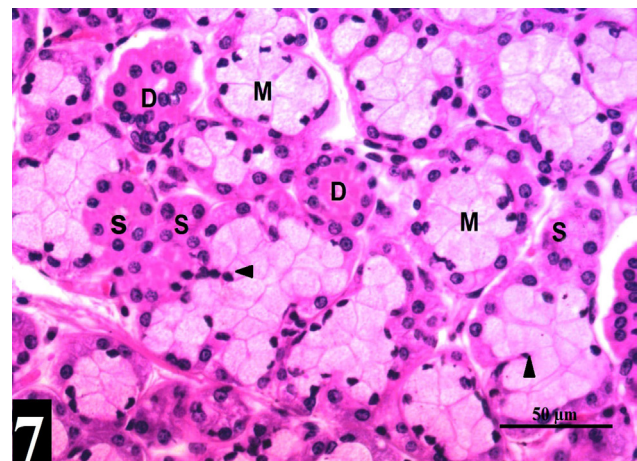


**Fig. 7:** A photomicrograph of a section of submandibular gland from a furan +Clove extract treated rat (group IV) showing regular acinar patterns with normal serous acini (S), mucous acini (M) and duct system (D). However, few desquamated nuclei (arrow head) in lumen of some mucous acini are still present. (H&E x 200).

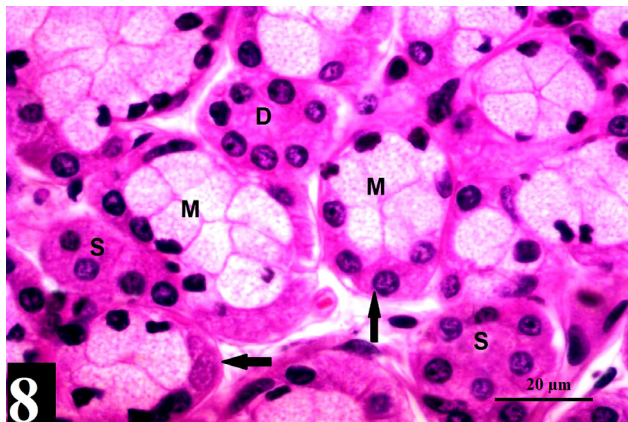


**Fig. 8:** A photomicrograph of a section of submandibular gland from a furan +Clove extract treated rat (group IV) showing that the gland restores its general normal architecture, having large pale staining mucous acini with foamy cytoplasm (M), serous acini with darkly stained cytoplasm (S), serous demilunes (arrow) and normal duct system (D). (H&E x 400).

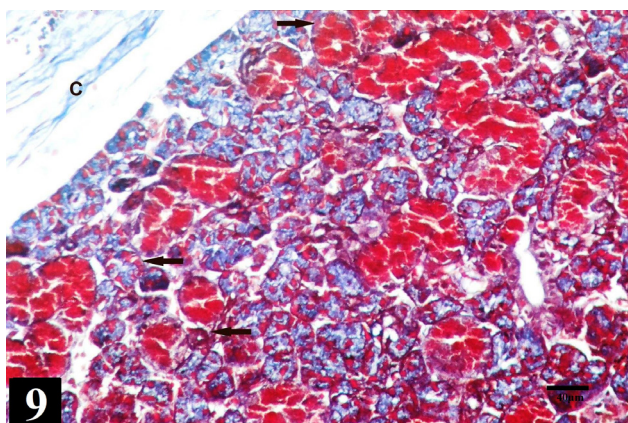


**Fig. 9:** A photomicrograph of a section of submandibular gland from a control rat [group I] showing thin connective tissue capsule [C] and minimal amount of collagen fibers around the acini and the ducts [arrows]. [Mallory trichrome x 200]

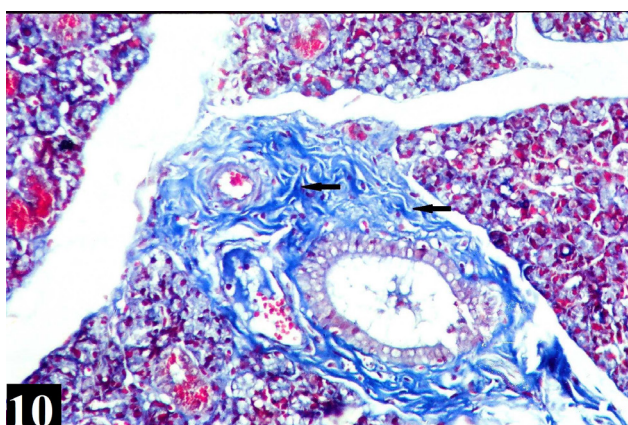


**Fig. 10:** A photomicrograph of a section of submandibular gland from a furan treated rat (group III) showing excessive periductal and perivascular accumulation of collagen fibers (arrows). (Mallory trichrome x 200).

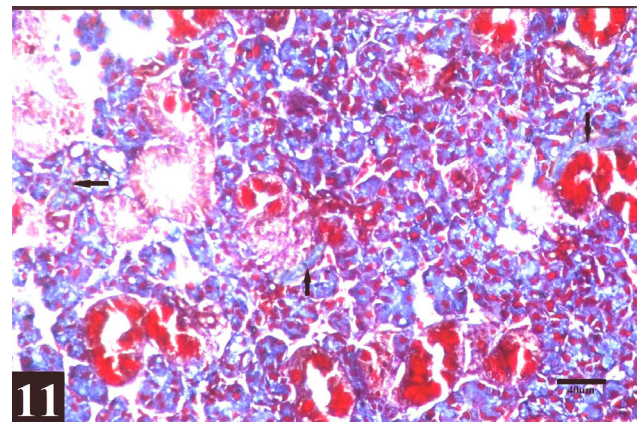


**Fig. 11:** A photomicrograph of a section of submandibular gland from a furan +Clove extract treated rat (group IV) displaying moderate amount of collagen fibers around the ducts and acini (arrows). (Mallory trichrome x 200).

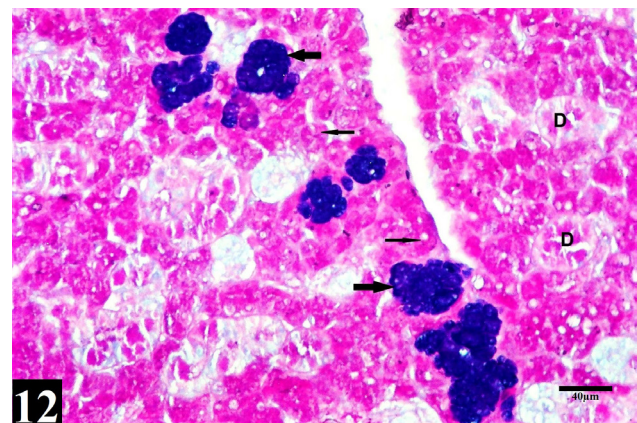


**Fig. 12:** A photomicrograph of a section of submandibular gland from a control rat (group I) showing strong PAS +ve response of the serous acini (thin arrows) and duct cells (D). The mucous acini display a clear blue reaction of Alcian blue (thick arrows). (Alcian blue – PAS x 200).

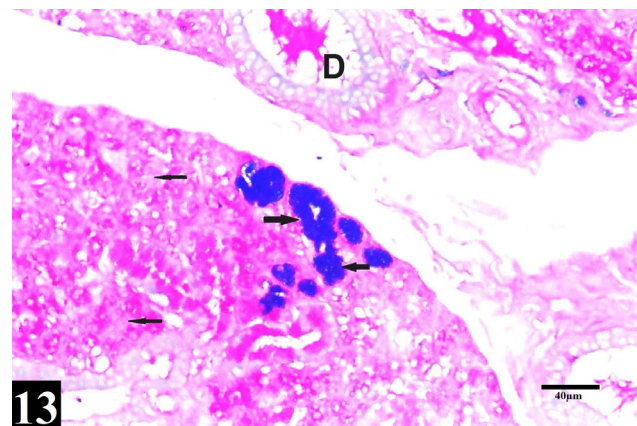


**Fig. 13:** A photomicrograph of a section of submandibular gland from a furan treated rat (group III) showing weak serous acini PAS +ve reaction (thin arrows), moderate Alcian blue +ve mucus acini (thick arrows) and weak Alcian blue +ve duct reaction (D). (Alcian blue – PAS x 200).

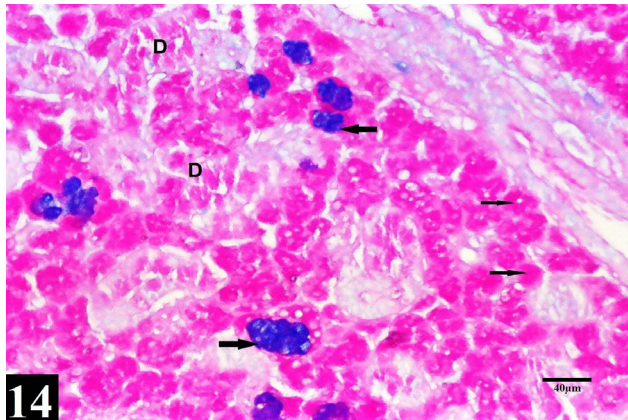


**Fig. 14:** A photomicrograph of a section of submandibular gland from a furan +Clove extract treated rat (group IV) showing moderate to heavy PAS + ve reaction of the serous acini (thin arrows) and ducts (D) whereas mucous acini shows moderate Alcian blue + ve reaction (thick arrows). (Alcian blue – PAS x 200).

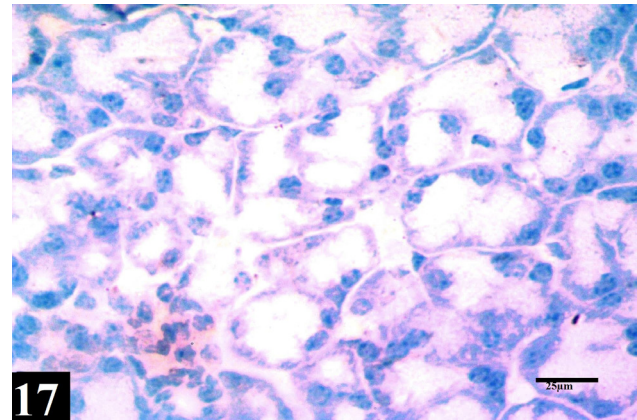


**Fig. 17:** A photomicrograph of a section of submandibular gland from a furan +Clove extract treated rat (group IV) showing negative Caspase-3 immune reactions of acinar cells. (Caspase -3 immunohistochemistry x 400).

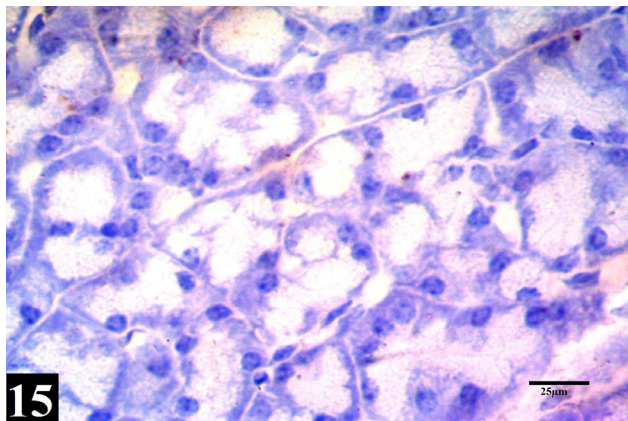


**Fig. 15:** A photomicrograph of a section of submandibular gland from a control rat (group I) showing negative acinar cell immunoreactivity of Caspase-3. (Caspase -3 immunohistochemistry x 400).

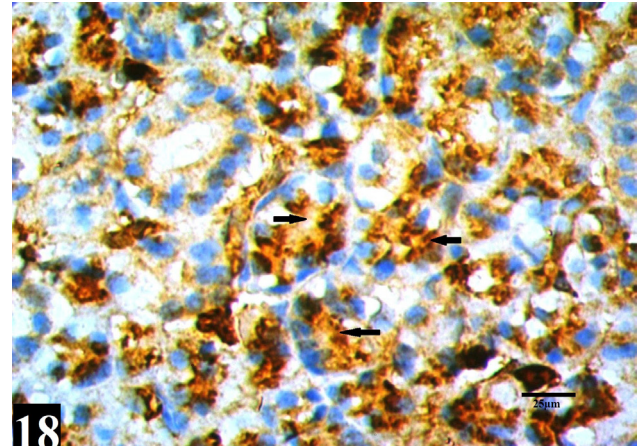


**Fig. 18:** A photomicrograph of a section of submandibular gland from a control rat (group I) showing strong positive cytoplasmic CYP2E1 expression in the acini (arrows). (CYP2E1 immunohistochemistry x 400).

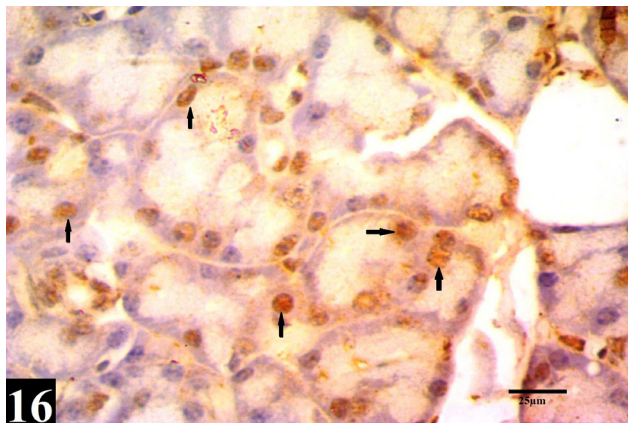


**Fig. 16:** A photomicrograph of a section of submandibular gland from a furan treated rat (group III) showing strong positive nuclear immunoreaction of Caspase-3 in acinar cells (arrows) and weak cytoplasmic reaction. (Caspase -3 immunohistochemistry x 400).

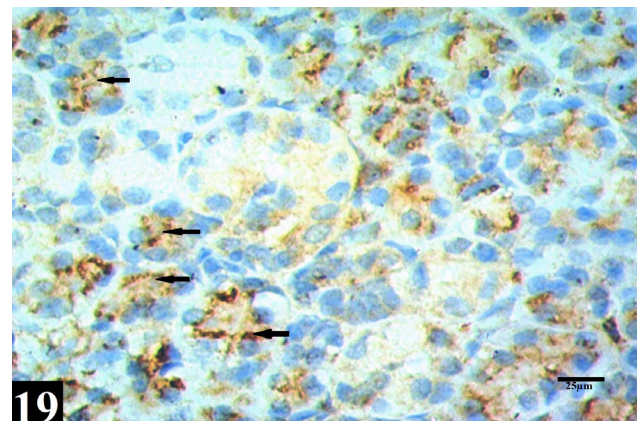


**Fig. 19:** A photomicrograph of a section of submandibular gland from a furan treated rat (group III) showing mild positive cytoplasmic CYP2E1 expression in the acini (arrows). (CYP2E1 immunohistochemistry x 400).

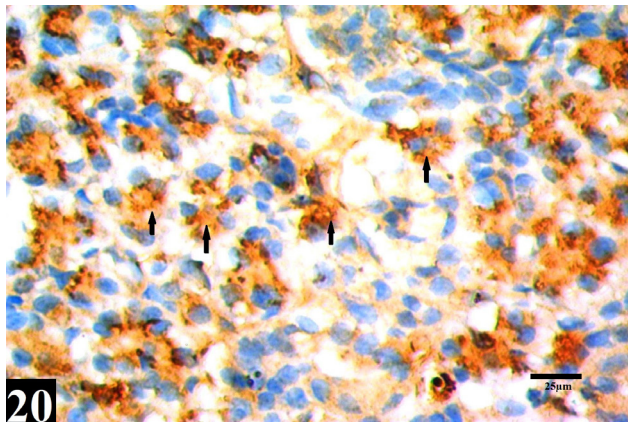


**Fig. 20:** A photomicrograph of a section of submandibular gland from a furan +Clove extract treated rat (group IV) showing moderate positive cytoplasmic CYP2E1 immunoreaction of the acini (arrows). (CYP2E1 immunohistochemistry x 400).

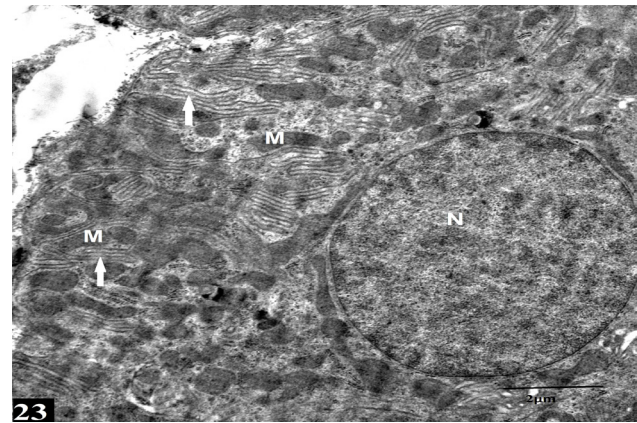


**Fig. 23:** An electron micrograph of submandibular gland from a control rat (group I) showing the basal part of a striated duct cell with rounded euchromatic nucleus (N), infolding of the basal membrane (arrows) and mitochondria (M) in between. (TEM x 14000).

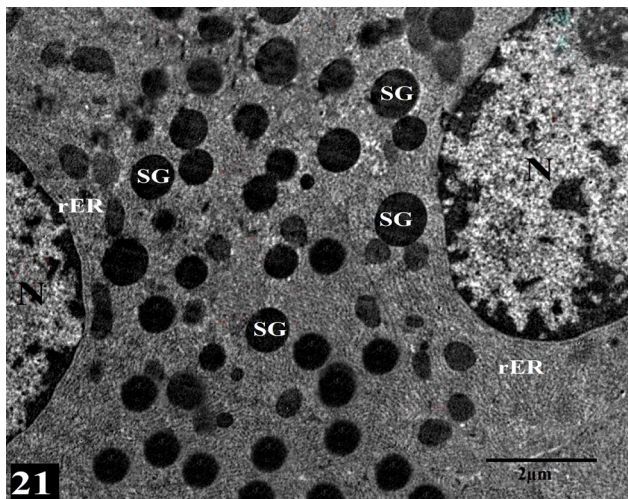


**Fig. 21:** An electron micrograph of submandibular gland from a control rat (group I) showing serous secreting acinar cells having regular euchromatic nuclei (N), basal and perinuclear cisternae of rough endoplasmic reticulum (rER) and supranuclear homogenous electron-dense secretory granules (SG). (TEM x 8000).

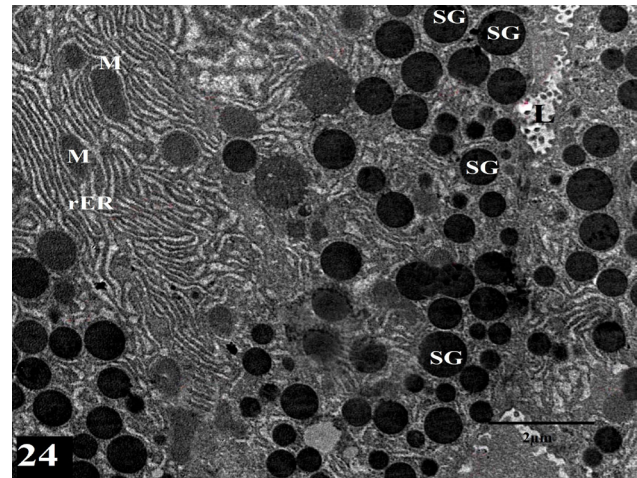


**Fig. 24:** An electron micrograph of the submandibular gland of a Furan treated rat (group III) showing serous acinar cells having electron dense granules (SG), dilated cisternae of rough endoplasmic reticulum (rER) and degenerated mitochondria (M). Note the lumen of the acinus (L). (TEM x 8000).

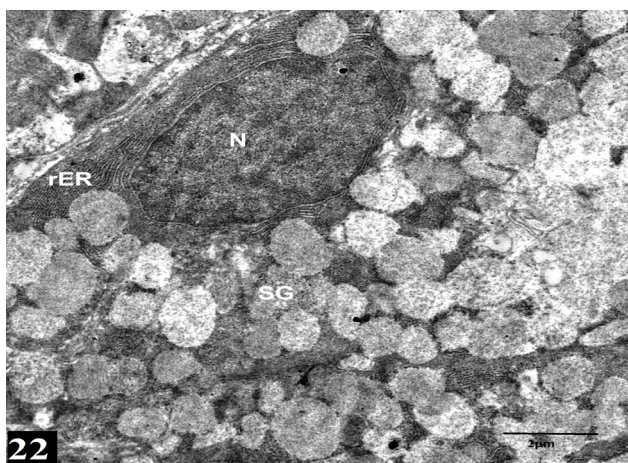


**Fig. 22:** An electron micrograph of submandibular gland from a control rat (group I) showing mucous acinus cell with basal oval nucleus (N), basal cisternae of rough endoplasmic reticulum (rER) and apical electron-lucent secretory granules (SG) of variable sizes and filling most of the cytoplasm. (TEM x 14000).

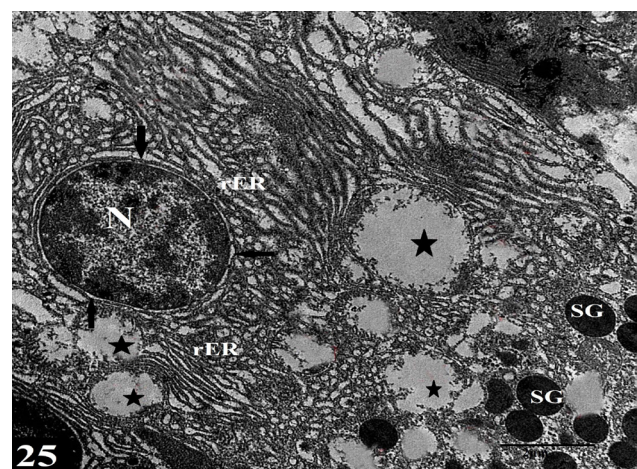


**Fig. 25:** An electron micrograph of the submandibular gland of a Furan treated rat (group III) showing serous acinar cells with more condensed nuclear chromatin (N), dilated perinuclear space (arrow) and rough endoplasmic reticulum (rER). The secretory granules are heterogenous and showed apparent decrease. Some contents appeared dense (SG) while others were lucent (star). (TEM x 8000).

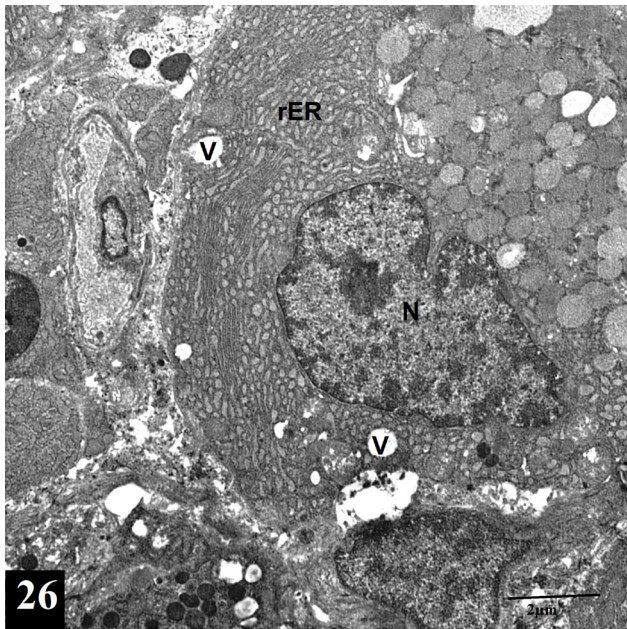


**Fig. 26:** An electron micrograph of the submandibular gland of a Furan treated rat (group III) showing mucous acinar cell having vacuolated cytoplasm (V), irregular indented nucleus (N) and dilated cisternae of rough endoplasmic reticulum (rER). (TEM x 8000).

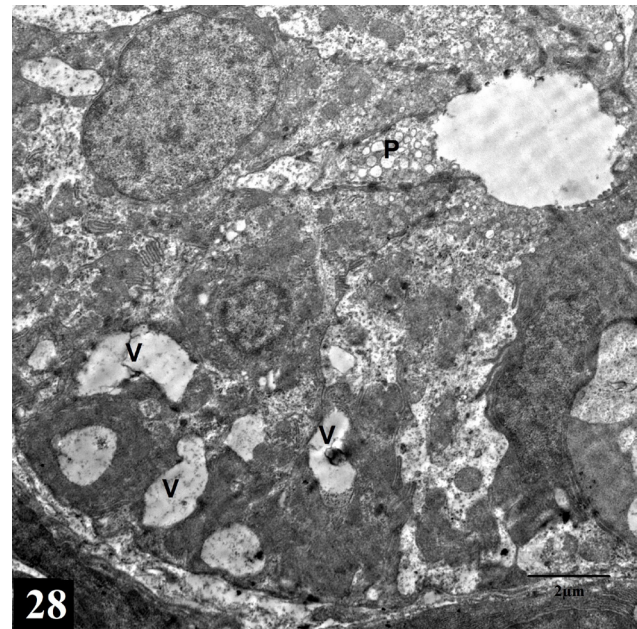


**Fig. 28:** An electron micrograph of the submandibular gland of a Furan treated rat (group III) showing striated duct cells having loss of normal architecture. Multiple cytoplasmic vacuoles (V), apical pinocytotic vesicles (P) with loss of basal membrane infoldings are observed. (TEM x 8000).

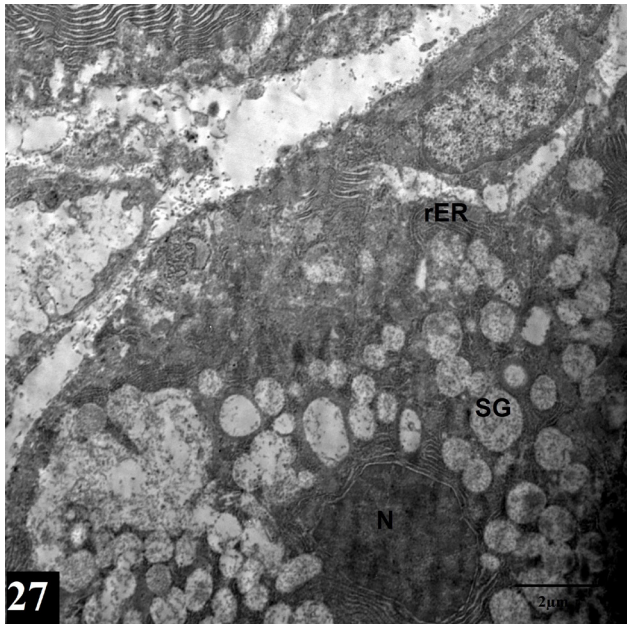


**Fig. 27:** An electron micrograph of the submandibular gland of a Furan treated rat (group III) showing mucous acinar cell showed secretory granules (SG) with basal migration of some of them (arrows). Notice the nucleus (N) and slightly dilated cisternae of rough endoplasmic reticulum (rER). (TEM x 8000).

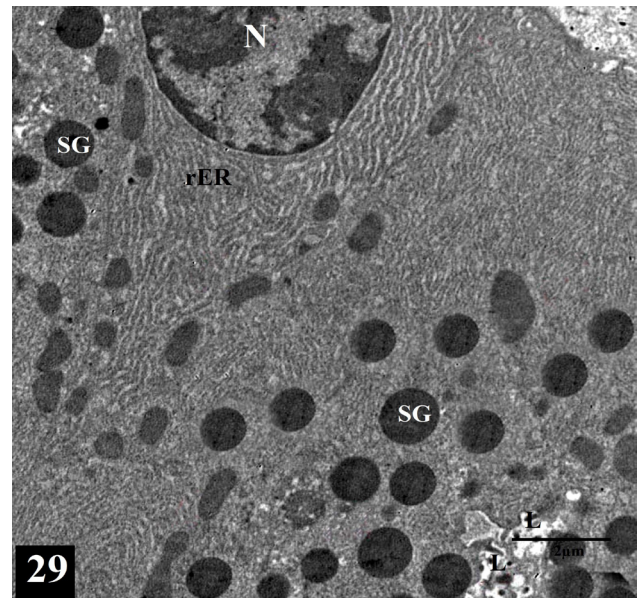


**Fig. 29:** An electron micrograph of the submandibular gland of a Furan +Clove extract treated rat (group IV) showing serous acinar cells with euchromatic regular nuclei (N), apical dense secretory granules (SG) with intact intercellular junctions (J). However, rough endoplasmic reticulum showed mild dilatation (rER). (TEM x 8000).

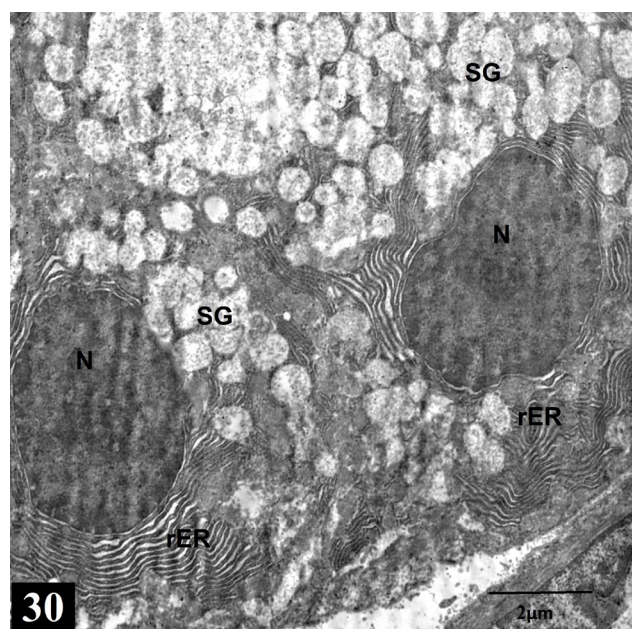


**Fig. 30:** An electron micrograph of the submandibular gland of a Furan +Clove extract treated rat (group IV) showing mucous acinar cells having nearly regular nuclei (N), with perinuclear and basal rough endoplasmic reticulum cisternae, (rER), and electron lucent supranuclear secretory granules (SG) Some cisternae of rough endoplasmic reticulum still dilated (arrow). (TEM x 8000).

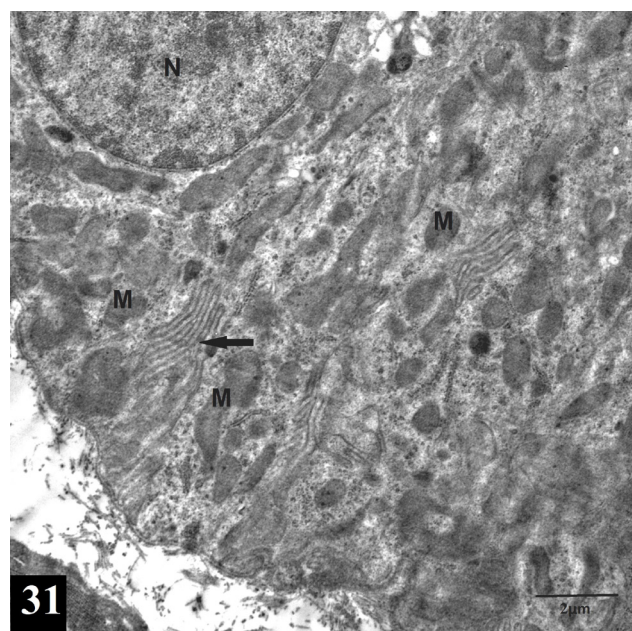


**Fig. 31:** An electron micrograph of the submandibular gland of a Furan +Clove extract treated rat (group IV) showing striated duct cell having an euchromatic nucleus (N), almost regular infoldings (arrows) with presence of mitochondria in between (M). (TEM x14000).

**Table 1:** Effect of different treatments on tissue levels of MDA, SOD and CAT of all groups of rats

Group	MDA (nmol/mg protein) $\bar{x} \pm SD$	SOD (U/mg protein) $\bar{x} \pm SD$	CAT (U/mg protein) $\bar{x} \pm SD$
Control group	2.2 ± 0.3	2.8 ± 0.5	137.4 ± 2.9
Clove extract group	2.4 ± 0.3	3.0 ± 0.4	140.3 ± 4.0
Furan treated group	23.5 ± 2.3**	0.4 ± 0.1**	31.3 ± 2.8**
Furan+Clove extract group	8.3 ± 1.3**	1.2 ± 0.2**	103.3 ± 3.8**

$\bar{x}$  = the mean value. SD= the standard deviation.

\* Significant at  $P < 0.05$  compared with control group

\*\* highly significant from the control group ( $p < 0.001$ ).

♦ Significant from the Furan treated group ( $p < 0.05$ )

♦♦ highly significant from Furan treated group ( $p < 0.001$ )

**Table 2:** Mean surface area percentage (%) of collagen fiber deposition in different experimental groups

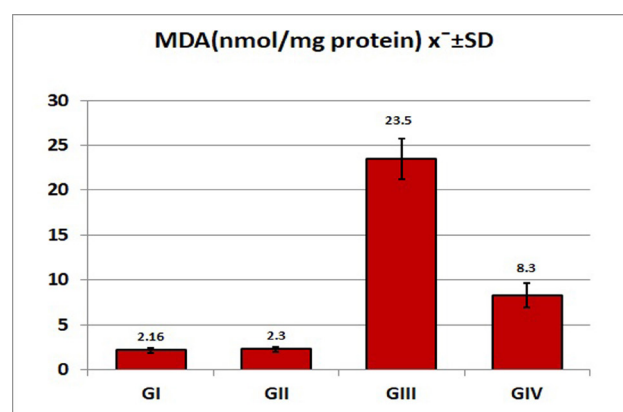
Experimental groups	Collagen-fiber mean area percentage (%) $\bar{x} \pm SD$
Control group (group I)	12.2 ± 0.3
Clove extract group (group II)	11.9 ± 0.6
Furan –treated group (group III)	39.1 ± 0.9**
Furan +Clove extract group (Group IV)	22.3 ± 1.7**

$\bar{x}$  = the mean value. SD= the standard deviation.

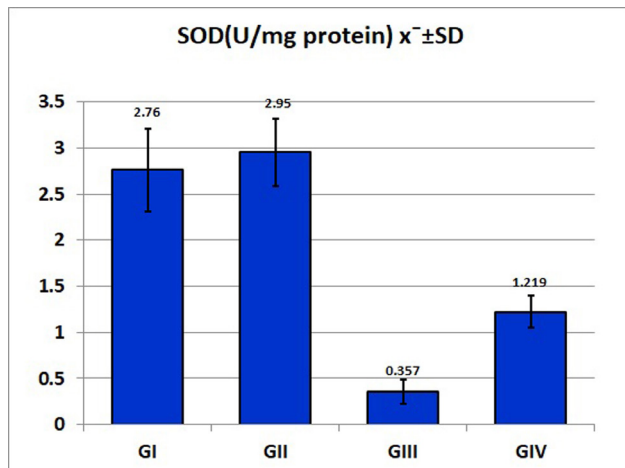
\*\* Highly significant from the control group ( $p < 0.001$ ).

♦ Significant from Furan –treated group ( $P < 0.05$ )

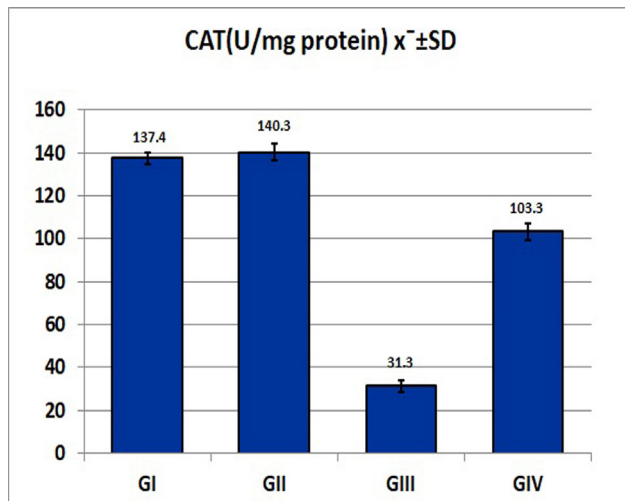
♦♦ highly significant from Furan treated group ( $p < 0.001$ )



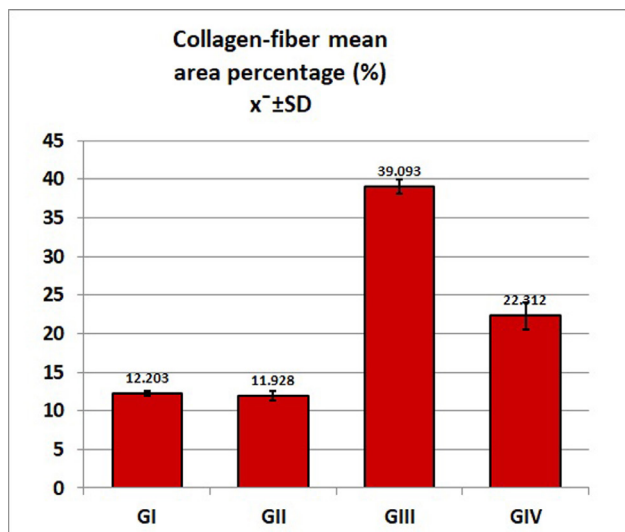
**Histogram 1:** Effect of different treatments on tissue levels of MDA, SOD and CAT of all groups of rats



**Histogram 2:** Effect of different treatments on tissue levels of MDA, SOD and CAT of all groups of rats



**Histogram 3:** Effect of different treatments on tissue levels of MDA, SOD and CAT of all groups of rats



**Histogram 4:** Collagen fibers mean area percentage

## DISCUSSION

Furan is a food pollutant which affects the health of the community harmfully. However, the effects of furan on the liver<sup>[7]</sup>, pancreas and endocrine system have been documented in a number of several studies<sup>[9]</sup>. Few studies have examined its effect on the salivary glands. So, the noxious effect of furan on submandibular rat salivary glands has been explained in the current report.

In the current research, animals treated with Furan revealed a distortion of the gland's histological architecture. Disorganized degenerated acini with vacuolations and enlarged hyperchromatic nuclei in acinar cells and interlobular duct cell have been observed. Loss of the typical parenchymal architecture could be explained by Ali *et al*<sup>[29]</sup> who mentioned that degeneration is a disturbance in the metabolism of the cell resulting in morphologic abnormalities. Thus, the cells could lose their normal architectural pattern of arrangement. These changes were in agreement with<sup>[10]</sup> who reported that furan induced degeneration, and distortion of the pancreatic exocrine acinar cells. In this work, these glandular damage and dysfunction caused by administration of Furan; the dioxin-like compounds (2, 3, 4, 7, 8-Pentachlorodibenzofuran)<sup>[30]</sup>. In accordance with Kiukkonen *et al*<sup>[31]</sup> who demonstrated that Dioxin toxicity increased epithelial apoptosis in developing salivary gland. Furan and its derivatives are cytotoxic and cause pathological changes as in previous study on liver and kidney<sup>[32]</sup>.

Periductal cellular infiltration and congested blood vessels were observed in the current research. These results were consistent with El Habiby *et al*.<sup>[10]</sup> who stated that furan induced cell invasion, blood vessel obstruction, and cytoplasmic vacuolation of rat pancreatic acinar cells. Karacaoglu *et al*<sup>[33]</sup> also reported that in furan-administered rats, acinar cell necrosis and vascular congestion were detected in the exocrine part of the pancreas. It was clarified as follow; Furan induces nitric oxide. The induced toxic effect of nitric oxide on submandibular acinar cells may be increased and vascular obstruction may increase<sup>[34]</sup>. In addition, blood vessel dilatation and congestion could be due to microcirculatory disruptions occurring as a side effect of Furan toxicity<sup>[35]</sup>. The lipid peroxidation and accumulation of oxygen dependent free radicals may explain the cellular infiltration observed after treatment with furan<sup>[36]</sup>. Furthermore, Wu *et al*<sup>[37]</sup> stated that by increasing cytokine expression and macrophage activation, Furan could induce cellular infiltration and inflammatory response.

As regards the occurrence of acinar and duct cell cytoplasmic vacuolations. Robbins *et al*<sup>[38]</sup> explained that vacuoles represent a cellular reaction against the noxious agents in which these materials have been accumulated in the vacuoles, thereby blocking their cellular metabolic process intervention. Irregular indented nuclei, degenerated mitochondria, dilatation of rER cisterns and loss of basal membrane infolding were suggested as signs of toxicity<sup>[39]</sup>.

Overproduction of ROS in relation with furan toxicity leads to oxidative stress, cellular damage, and necrosis caused by several mechanisms including peroxidation of membrane lipids, protein denaturation, and DNA damage<sup>[40]</sup>.

The reduction in secretory granules with basal migration in some cells in this work are explained by El-Agamy *et al*, as follow<sup>[41]</sup>; RER dilatation may resulting from cell injury due to disorganization of integral membrane protein and cytoskeleton or a result of deficiency of the protective enzymes, superoxide dimutase and glutathione peroxidase. As the rER is the main site of protein synthesis, so, any disruption in rER leads to an altered producing mechanism with subsequent degranulation or reduction of secretory granules. Reduction of secretory granules was preceded by their basal migration due to arrest of exocytosis enhancing basolateral release of granules.

A large increase in periductal and perivascular collagen fibers was observed in our research. This was in agreement with Menezes *et al*<sup>[42]</sup>, who stated that, irrespective of its cause, excessive increases in collagen fibers can repair extended tissue harm. Therefore, the increase in deposition of collagen fibers in our sample was caused by the subsequent injury after administration of Furan. The excessive fibrosis around the ducts and blood vessels may therefore be due to Furan's toxic effect.

Caspase-3 expression was increased in most acinar cells after furan treatment in the current study. Hickling *et al*<sup>[43]</sup> suggested that during the time of treatment with furan, apoptosis increased in the liver. Soliman *et al*<sup>[44]</sup> explained that apoptosis may be caused by activation of the procaspase-12 initiator, which is activated by cleavage under endoplasmic reticulum stress conditions, caused by oxidative stress, and can then activate caspases-9 and caspases-3, which induce apoptosis.

CYP2E1, primarily located in the liver, is involved in the metabolizing and activation of many important toxic substances such as furan. It is also expressed in rabbit, mouse, rat and human submandibular acinar and ductal cells<sup>[45]</sup>. The toxicity of furan is mediated by catalysis of cytochrome P450 (CYP2E1), which is responsible for furan oxidation<sup>[46]</sup>. Cis-2-butene-1,4-dial BDA; BDA is the primary product of CYP-catalyzed oxidation of furan and is responsible for the toxic effects of furan causing cytotoxicity and oxidative stress<sup>[11]</sup>. Furan treatment was found to decrease CYP2E1 expression in submandibular acini in our study. This was in accordance with Hickling *et al*<sup>[43]</sup>, who showed that hepatocyte expression of CYP2E1 was decreased during furan therapy. The decrease in CYP2E1 expression may be due to the ubiquitin-dependent proteasomal degradation mechanism UPS<sup>[47]</sup> post-translational degradation of CYP2E1. It can be concluded that in our sample, the furan-induced oxidative stress was due to activation of CYP2E1 that could be extensively consumed during the bio-activation phase of furan and underwent proper post-translational degradation by UPS.

Biochemical results showed a substantial increase in the MDA submandibular gland and a decrease in the levels of SOD and CAT in the in furan-treated groups compared with the control groups, indicating that furan-induced oxidative stress. These results were coincided with Wang *et al*<sup>[48]</sup> who reported decrease in the emission of SOD and GSH and an increase in the level of MDA in the liver and kidney of furan-treated mice.

Co-administration of Clove extract to furan-treated rats, however, showed a marked decrease in submandibular gland pathological changes, and the gland 'architecture, structure of acinar cells and duct system were apparently as in control animals. The previous data were in line with Shukri *et al*<sup>[49]</sup> who stated that dietary cloves in diabetic rats had decreased oxidant activities (Superoxide dismutase - Glutathione peroxidase - Catalase activity). Cloves are rich in antioxidant components that can relieve oxidative stress, including eugenol and vitamin C. Clove extract's active ingredient, like eugenol, reduces inflammation and oxidative stress. Eugenol has been reported to stimulate the activity of antioxidant enzymes such as superoxide dismutase (SOD), catalase (CAT), glutathione peroxidase (GPx), glutathione-S-transferase (GST) and polyphenol oxidase (PPO), which, by reducing oxidative stress, also preserves cell organelles<sup>[19]</sup>. The protective effects of clove extract on the hepatotoxicity of H<sub>2</sub>O<sub>2</sub>-induced rats appear to be linked to lipid peroxidation suppression and the removal of free radicals<sup>[50]</sup>.

Similarly, Palanivel *et al*<sup>[51]</sup> explained that the antioxidant and hepato-protective activities are the responsibility of polyphenolic compounds and flavanoids present in clove extract.

Similar findings by Yadav and Bhatnagar<sup>[52]</sup>, who showed in rat liver homogenate, cloves bud extract showed the highest radical scavenging activity due to its major aroma components, eugenol and eugenol acetate, induced substantial elevation in the magnitude of SOD and CAT with a concomitant reduction in MDA levels.

The antioxidant potential of cloves could benefit from a higher content of organic phenol compounds such as eugenol and eugenyl acetate and their ability to donate hydrogen, which are known to be strong free radical scavengers<sup>[53]</sup>.

It is concluded that administration of Clove extract to Furan treated rats could improve the histological, biochemical and immunohistochemical abnormalities of the submandibular gland from all the data and results reported. Considering these findings, Cloves mediated the protective effect to Furan` toxicity and could have a potential health benefit and consequently improvement in the quality of life. However, advanced investigations are needed to understand potential usefulness of this plant as a source of protective agent against Furan induced submandibular damage in clinical trials.

**CONFLICT OF INTERESTS**

There are no conflicts of interest.

**REFERENCES**

- Perez-Locas C, Yaylayan VA (2004): Origin and mechanistic pathways of formation of the parent furan – a food toxicant. *J Agric Food Chem.* 52(22): 6830–6836.
- Vranova' J, Ciesarova' Z (2009): Furan in food – a review. *Czech J. Food Sci.* 27(1): 1–10.
- Becalski A, Seaman S (2005): Furan precursors in food: A model study and development of a simple headspace method for determination of furan. *Journal of AOAC International.* 88: 102–106.
- Bakhiya N, Appel K E (2010): Toxicity and carcinogenicity of furan in human diet. *Arch Toxicol.* 84: 563–578.
- EFSA (European Food Safety Authority) (2017): Risks for public health related to the presence of furan and methylfurans in food. EFSA Panel on Contaminants in the Food Chain (CONTAM). *EFSA Journal.* 15(10):5005.
- Hamadeh HK, Jayadev S, Gaillard ET, Huang Q, Stoll R, Blanchard K, Chou J, Tucker CJ, Collins J, Maronpot R, Bushel P, Afshari C A (2004): Integration of clinical and gene expression endpoints to explore furan-mediated hepatotoxicity. *Mutat Res.* 549 (1-2):169–183.
- Kaya E, Yilmaz S, Ceribasi S (2019): Protective role of propolis on low and high dose furan-induced hepatotoxicity and oxidative stress in rats. *J Vet Res.* 63(3):423-431.
- Clement RE, Tosine HM, Taguchi V, Musial CJ, Uthe JF (1987): Investigation of American lobster, *Homarus americanus*, for the presence of chlorinated dibenzo-p-dioxins and dibenzofurans. *Bull Environ Contam Toxicol.* 39 (6): 1069–1075..
- Santokh G, Meghan K, Wendy C, Michael B, Madeline W, Gerard MC (2015): A 28-day Gavage Toxicity Study in Fischer 344 Rats with 3-methylfuran. *Toxicologic Pathology.* 43 (2): 221-232.
- El Habiby M M, El Sherif N M, El-Akabawy G, Sara GT (2017): Protective effect of garlic oil on furan induced damage in the pancreas of adult male rat, *Menoufia Medical Journal.* 30 (1): 262–270.
- Peterson L A, Cummings M E, Chan JY, Vu C C, Matter B A (2006): Identification of a cis-2-butene-1, 4-dial-derived glutathione conjugate in the urine of furan-treated rats. *Chem Res Toxicol.* 19 (9): 1138–1141.
- Jirovetz L, Buchbauer G (2006): Chemical Composition and Antioxidant Properties of Clove Leaf Essential Oils. *Journal of Agricultural and Food Chemistry.* 54 (17):6303-6307.
- Kumar U, Kumar B, Bhandari A, Kumar Y (2010): Phytochemical investigation and comparison of antimicrobial screening of clove and cardamom. *International Journal of Pharmaceutical Science and Research.*; 1(12): 138- 147.
- Sahu S, Sahoo A K, Swain S, Bhattacharyay D (2020): In silico Analysis of Phytochemicals from Clove against Bronchitis. *European Journal of Medicinal Plants.*; 31(5): 34-39.
- Debjit B K P, Sampath K, Akhilesh Y, Shweta S, Shravan P, Amit SD (2012): Recent Trends in Indian Traditional Herbs *Syzygium aromaticum* and its Health xd
- Ghadermazi R, Keramat J, Goli SA (2017): Antioxidant activity of clove (*Eugenia caryophyllata* Thunb), oregano *Origanum vulgare* L and sage (*Salvia officinalis* L) essential oils in various model systems. *International Food Research Journal.* 24(4): 1628-1635.
- McDanie LP, Ding W, Dobrovolsky VN, Shaddock JG, Mittelstaedt RA, Doerge DR, Heflich RH (2012): Genotoxicity of furan in Big Blue rats. *Mutat Res.*; 742 (1-2) :72–78.
- Moro S, Chipman JK, Wegener JW, Hamberger C, Dekant W, Mally A (2012): Furan in heat treated foods: formation, exposure, toxicity, and aspects of risk assessment. *Mol Nutr Food Res.*; 56:1197–1211.
- Abozid M M, EL-Sayed SM (2013): Antioxidant And Protective Effect Of Clove Extracts And Clove Essential Oil On Hydrogen Peroxide Treated Rats, *International Journal of Chem Tech Research.* 5 (4) : 1477-1485.
- Bancroft Jd and Gamble M (2013): Theory and practice of histological techniques. 7th ed., Churchill Livingstone/Elsevier, Oxford. 173-179, 363-39.
- Kiernan J A (2015): Histological and histochemical methods; Theory and practice. 5th ed : 238-390.
- Ramos-Vara JA, Kiupel M, Baszler T (2008): American association of veterinary laboratory diagnosticians subcommittee on standardization of immunohistochemistry: Suggested guidelines for immunohistochemical techniques in veterinary diagnostic laboratories. *J Vet Diagn Invest.* 20(4): 393–413.
- Sabry MM, Elkalawy SAE, Abo-Elnour RKD (2014): Histological and immunohistochemical study on the effect of stem cell therapy on bleomycin induced pulmonary fibrosis in albino rat. *Int J Stem Cells.* 7(1): 33–42.
- Dykstra K, Michael J, Laura E (2003): Biological Electron Microscopy Theory, Techniques, and Troubleshooting effect of vitamin E and vitamin C. *Pest Biochem Physiol.* 118:10–18.

25. Wills E (1987): Evaluation of lipid peroxidation in lipids and biological membranes. In: Mullock B, Snell K editor Biochemical toxicology, a practical approach. Oxford, UK: IRL Press.; 127–152.
26. Aebi H (1984): Catalase in *vitro*. *Methods Enzymol.*; 105:121–126.
27. Gloria E, Borgstahl O, Rebecca E (2018). Superoxide Dismutases (SODs) and SOD Mimetics. *Antioxidants*, 7(11): 156.
28. Peat J and Barton B (2005): Medical statistics. A Guide to data analysis and critical appraisal. First Edition. Wiley-Blackwell:113-19.
29. Ali KA, Elbolok HA, Mohamed SD (2016): Histological and immunohistochemical evaluation of the possible effects of different doses of caffeine on submandibular salivary gland of adult male albino rats using (ANNEXIN A5) marker. *Egyptian Dental Journal*. 62 (1): 635-43. I.S.S.N 0070-9484.
30. Walker NJ, Crockett PW, Nyska A (2005): Dose additive carcinogenicity of a defined mixture of "dioxin-like compounds". *Environ Health Perspect.*; 113: 43–48.
31. Kiukkonen A1, Sahlberg C, Partanen AM, Alaluusua S, Pohjanvirta R, Tuomisto J, Lukinmaa PL (2006): Interference by 2,3,7,8-tetrachlorodibenzo-p-dioxin with cultured mouse submandibular gland branching morphogenesis involves reduced epidermal growth factor receptor signaling. *Toxicol Appl Pharmacol.*; 212(3):200-11.
32. Yuan Y, Wu SJ, Liu X, Zhang LL (2013). Antioxidant effect of salidroside and its protective effect against furan-induced hepatocyte damage in mice. *Food Funct*. 4: 763–769
33. Karacaoglu E, Selmanoglu G, Kilic A (2012): Histopathological effects of the food contaminant furan on some endocrine glands of prepubertal male rats. *Turk J Med Sci*. 42 (1):1207–1213.
34. Nyska A, Jokinen MP, Brix AE, Sells DM, Wyde ME, Orzech D (2004): Exocrine pancreatic pathology in female Harlan Sprague-Dawley rats after chronic treatment with 2,3,7,8-tetrachlorodibenzo-p-dioxin and dioxin-like compounds. *Environ Health Perspect*. 112 (8): 903–909.
35. Kara O (2015): Toxicity of furan on testis in diabetic rats and protective role of lycopene, Master Thesis, Bozok University/Graduate School of Natural and Applied Sciences.; Department of Biology, promoter D. Pandir.
36. Reuter S, Gupta SC, Chaturvedi MM, Aggarwal BB (2010): Oxidative stress, inflammation, and cancer: how are they linked? *Free Radic Biol Med.*; 49 (11):1603–1616.
37. Wu L, Song Y, Xu X, Li N, Shao M, Zhang H (2014): Medium-assisted non-polar solvent dynamic microwave extraction for determination of organophosphorus pesticides in cereals using gas chromatography-mass spectrometry. *Food Chem*. 162:253–260.
38. Robbins S L, Cotran R S, Kumar V (1984): *Pathologic Basis of Disease* (3<sup>rd</sup> ed.). Philadelphia, PA: W.B. Saunders.
39. Mohammed SS, El-Sakhawy M A, Sherif H, Shredah, M (2015): Effect of Aspartame on Submandibular Salivary Glands of Adult Male Albino Rats. *Life Sci J*; 12(3):44-50.
40. Hickling KC, Hitchcock JM, Oreffo V, Mally A, Hammond TG, Evans JG, Chipman J K. (2010): Evidence of oxidative stress and associated DNA damage, increased proliferative drive, and altered gene expression in rat liver produced by the cholangiocarcinogenic agent furan. *Toxicol Pathol*, 38, 230–243.
41. El-Agamy AA, Afifi OK, Sheta AA (2014): Protective Role of Panax Gensing on Fluvoxamine Maleate Induced Structural Changes in the Submandibular Salivary Gland of Rats. *Nature and Science*; 12(4).
42. Menezes S L, Bozza PT, Neto HC, Laranjeira A P, Negri E M, Capelozzi V L, Zin W A (2005): Pulmonary and Extra Pulmonary Acute Lung Injury. *J. Applied. Physiol*. 98(5): 1777-1778.
43. Hickling KC, Hitchcock JM, Chipman JK, Hammond TG, Evans JG. (2010): Induction and progression of cholangiofibrosis in rat liver injured by oral administration of furan. *Toxicol Pathol*. 38:213–229.
44. Soliman ME, Kefafy MA, Mansour MA, Ali AF, Esa WA (2014): Histological study on the possible protective effect of pentoxifylline on pancreatic acini of l arginine induced acute pancreatitis in adult male albino rats. *Menouf Med J*. 27:801–808.
45. Coon MJ (2005): Cytochrome P450: nature's most versatile biological catalyst. *Annu Rev Pharmacol Toxicol*; 45: 1–25.
46. Jackson AF, Williams A, Recio L, Waters MD, Lambert IB, Yauk CL (2014): Case study on the utility of hepatic global gene expression profiling in the risk assessment of the carcinogen furan. *Toxicol Appl Pharmacol*; 274:63–77.
47. Zhang CL, Zeng T, Zhao XL, Xie KQ (2013): Garlic oil attenuated nitrosodiethylamine induced hepatocarcinogenesis by modulating the metabolic activation and detoxification enzymes. *Int J Biol Sci*; 9:237–245.
48. Wang E, Chen F, Hu X, Yuan Y (2014): Protective effects of apigenin against furan induced toxicity in mice. *Food Funct.*; 5 (8):1804–1812.

49. Shukri R, Mohamed S, and Mustapha N M (2010): Cloves protect the heart, liver and lens of diabetic rats. *Food Chem.*; 122 (4): 1116 – 1121.
50. Gulcin I, Sat IG, Beydemir S, Elmastas M, and Kufrevioglu OI (2004): Comparison of antioxidant activity of clove (*Eugenia caryophyllata* Thunb) buds and lavender (*Lavandulastoechas* L.) *Food Chemistry*.; 87(3): 393–400.
51. Palanivel M G, Raj Kapoor B, Kumar R S, Einstein J W (2008): Hepatoprotective and Antioxidant Effect of *Pisonia aculeata* L. against CCl<sub>4</sub>- Induced Hepatic Damage in Rats. *Sci Pharm.*; 76: 203–215.
52. Yadav AS, Bhatnagar D(2007): Free radical scavenging activity, metal chelation and antioxidant power of some Indian spices .*Biofactors*.; 31(3-4): 219-227.
53. Chaieb K, Zmantar T, Ksouri R, Hajlaoui H, Mahdouani K, Abdely C, Bakhrouf A (2007): Antioxidant properties of the essential oil of *Eugenia caryophyllata* and its antifungal activity against a large number of clinical *Candida* species. *Mycoses*.; 50 (5): 403-406.

## الملخص العربي

# التقييم النسيجي والكيميائي المناعي والكيميائي الحيوي للقدرة الوقائية للقرنفل ضد تغيرات الغدة اللعابية تحت الفك السفلي التي يسببها الفيوران في ذكور الجرذان البيضاء البالغة

هالة محمد الحرون، نادية سعيد بدوي خير

قسم الهستولوجيا، كلية الطب، جامعة المنوفية، مصر

**المقدمة:** الفيوران هو مركب من ملوثات الطعام المنتشرة على نطاق واسع في الهواء والماء والتربة والرواسب في جميع أنحاء العالم. وينشأ في الأطعمة المعلبة والمبسترة و المصنعة المعرضة للحرارة. يوجد أيضاً في دخان السجائر وكمركب وسيط في معالجة العديد من المنتجات الكيميائية والصيدلانية. يستخدم القرنفل في الطب الشعبي كتوابل للطعام وكعطور ومستحضرات صيدلانية. وهناك العديد من الفوائد الصحية للقرنفل فهو عامل مضاد للجراثيم ومضاد للفطريات ومطهر ومضاد للأكسدة.

**الهدف:** يهدف البحث الحالي لدراسة تأثير الفيوران على التركيب النسيجي للغدة اللعابية تحت الفك السفلي للذكور البالغة من الجرذان البيضاء ويختبر التأثير الوقائي الممكن لمستخلص القرنفل.

**المواد والطرق المستخدمة:** استخدمت الدراسة الحالية ٤٨ من ذكور الجرذان البيضاء البالغة. تم تقسيمها بشكل عشوائي إلى أربع مجموعات: المجموعة الضابطة ، المجموعة المعالجة بالقرنفل والتي تلقت ٥٠٠ مجم / كجم / يوم ، ٥ أيام / الأسبوع ، المجموعة المعالجة بالفيوران تلقت ٨ مجم / كجم ، ٥ أيام / الأسبوع ، ومجموعة الفيوران والقرنفل ، في نهاية الدراسة (٨ أسابيع). تم تخدير الحيوانات واستئصال كل من الغدة تحت الفك السفلي لعمل الاختبارات النسيجية والكيميائية النسيجية والكيميائية المناعية والفحص المجهر الإلكتروني. كما تم إجراء القياس المورفومتري والإحصاءات.

**النتائج:** بالإضافة إلى التراكم المفرط لألياف الكولاجين حول الأوعية والأوعية الدموية ، أظهرت الغدة تحت الفك السفلي التي عولجت بالفوران عدم انتظام وتكسر لخلايا الغدة وقنواتها. وكذلك تحلل في الشبكة الإندوبلازمية ، والميتوكوندريا متبوعة بفقدان الغشاء القاعدي المنطوي. كما زاد الفيوران من موت الخلايا المبرمج ونقص CYP٢E١ السيتوبلازمي. و زادت كمية الإنزيمات المضادة للأكسدة ، ديسموتاز الفائق (SOD) والكتلاز (CAT) والمالونديالديهيد (MDA) بشكل ملحوظ. وقد أدى استعمال مستخلص القرنفل الى حماية ملحوظة ضد هذه التغييرات ، مما أظهر تحسنات كبيرة في تركيب الغدة اللعابية تحت الفك السفلي.

**الاستنتاجات:** يمكن استنتاج أن القرنفل له تأثير وقائي ويقلل من سمية الفيوران علي الغدة اللعابية تحت الفك السفلي.